TASK REPORT

Physics-Based Prediction of Unexploded Ordnance Penetration into Granular Materials

Computer Laboratory for Granular Physics Studies

SERDP Project MR-2630

NOVEMBER 2018

Jae H. Chung, Ph.D.
Theodor Krauthammer, Ph.D.
University of Florida

Distribution Statement A
This document has been cleared for public release

SERDP
DOD ▪ EPA ▪ DOE

Page Intentionally Left Blank

REPORT DOCUMENTATION PAGE

Form Approved
OMB No. 0704-0188

The public reporting burden for this collection of information is estimated to average 1 hour per response, including the time for reviewing instructions, searching existing data sources, gathering and maintaining the data needed, and completing and reviewing the collection of information. Send comments regarding this burden estimate or any other aspect of this collection of information, including suggestions for reducing the burden, to Department of Defense, Washington Headquarters Services, Directorate for Information Operations and Reports (0704-0188), 1215 Jefferson Davis Highway, Suite 1204, Arlington, VA 22202-4302. Respondents should be aware that notwithstanding any other provision of law, no person shall be subject to any penalty for failing to comply with a collection of information if it does not display a currently valid OMB control number.
PLEASE DO NOT RETURN YOUR FORM TO THE ABOVE ADDRESS.

1. REPORT DATE *(DD-MM-YYYY)*	2. REPORT TYPE	3. DATES COVERED *(From - To)*
11/30/2018	SERDP Task Report	3/7/2016 - 11/15/2018

4. TITLE AND SUBTITLE
Physics-Based Prediction of Unexploded Ordnance Penetration into Granular Materials

Computer Laboratory for Granular Physics Studies

5a. CONTRACT NUMBER
16-P-0010

5b. GRANT NUMBER

5c. PROGRAM ELEMENT NUMBER

6. AUTHOR(S)
Jae Chung

5d. PROJECT NUMBER
MR-2630

5e. TASK NUMBER

5f. WORK UNIT NUMBER

7. PERFORMING ORGANIZATION NAME(S) AND ADDRESS(ES)
University of Florida
1949 Stadium Rd. Room 365
Gainesville, FL 32611

8. PERFORMING ORGANIZATION REPORT NUMBER
MR-2630

9. SPONSORING/MONITORING AGENCY NAME(S) AND ADDRESS(ES)
Strategic Environmental Research and Development Program
4800 Mark Center Drive, Suite 17D03
Alexandria, VA 22350-3605

10. SPONSOR/MONITOR'S ACRONYM(S)
SERDP

11. SPONSOR/MONITOR'S REPORT NUMBER(S)
MR-2630

12. DISTRIBUTION/AVAILABILITY STATEMENT
Distribution A; unlimited public release

13. SUPPLEMENTARY NOTES

14. ABSTRACT
The following presents drop tower test results of dry granular material subjected to the impact of rigid penetrator, with particular attention paid to observable quantities such as the maximum penetration depth of the impactor. Herein, physical specimens of granular media primarily consist of high-uniformity, spherical granules. The specimens are utilized in conjunction with specialized preparation procedures to achieve pre-determined, mechanically-stable granular assemblies. Namely, for the granular assemblies considered, pluviation processes are controlled for loading history to achieve optimally-uniform relative density states, i.e., initial, gravitational lithostatic stress conditions.

15. SUBJECT TERMS
Unexploded Ordnance, UXO, Granular Materials, Granular Physics

16. SECURITY CLASSIFICATION OF:			17. LIMITATION OF ABSTRACT	18. NUMBER OF PAGES	19a. NAME OF RESPONSIBLE PERSON
a. REPORT	b. ABSTRACT	c. THIS PAGE			Jae Chung
UNCLASS	UNCLASS	UNCLASS	UNCLASS	32	19b. TELEPHONE NUMBER *(Include area code)* 352-392-9537 ex. 1512

Page Intentionally Left Blank

This report was prepared under contract to the Department of Defense Strategic Environmental Research and Development Program (SERDP). The publication of this report does not indicate endorsement by the Department of Defense, nor should the contents be construed as reflecting the official policy or position of the Department of Defense. Reference herein to any specific commercial product, process, or service by trade name, trademark, manufacturer, or otherwise, does not necessarily constitute or imply its endorsement, recommendation, or favoring by the Department of Defense.

Page Intentionally Left Blank

ABSTRACT

The following presents drop tower test results of dry granular material subjected to the impact of rigid penetrator, with particular attention paid to observable quantities such as the maximum penetration depth of the impactor. Herein, physical specimens of granular media primarily consist of high-uniformity, spherical granules. The specimens are utilized in conjunction with specialized preparation procedures to achieve pre-determined, mechanically-stable granular assemblies. Namely, for the granular assemblies considered, pluviation processes are controlled for loading history to achieve optimally-uniform relative density states, i.e., initial, gravitational lithostatic stress conditions. For physical experimentation setups, statistically-homogeneous granular assemblies are determined to be an initial condition for dry granular media subjected to low-velocity impact by a rigid penetrator. To facilitate the fundamental understanding of scale-dependent granular behaviors, geotechnical centrifuge was used to produce in-situ penetration at prototype-scales in Task 3. Complimentarily, the drop tower tests of this sub-Task 4.4 are conducted, which test data would be useful for verification of the numerical simulation results.

In the future, the corresponding numerical analysis is to be performed and calibrated within a statistical margin of errors so as to model the laboratory experimentation as closely as possible without introduction of empiricism. Libraries of numerical granular matrices have been developed which correspond to the physical proppants utilized in the laboratory experiments. Because the proof-of-concept numerical models are based on the application of soft-particle dynamic theory (extended Hertzian and Mindlinian contact mechanics) to analyses of physical data of surface topography and grain-to-grain contact force-deformation, they are expansible to a wide range of empirical experiments which can be numerically simulated and calibrated based on direct measurements using drop tower experimental technology. In this way, microscopic laboratory tests assessing surface roughness and asperity distributions across the surface of individual grains can be integrated into the calculation of individual discrete element (grain scale) parameters such as normal and tangential contact stiffness, and scale-dependent frictional resistance, which ultimately determine the degree of penetration resistance as per levels of energy dissipation mechanisms. A parametric-sensitivity study at system scales is desired in order to catalogue and compare within the measurements of the scale effects. The present drop tower testing affirms the suitability of impact experiments and facilitates the conceptual design for impact resistance of granular soils. Therefore, a simplified analytical procedure, suitable for conceptual design purposes, for predicting the resulting dynamic response of granular soils in in-situ conditions can be developed if the research continues.

TABLE OF CONTENTS

REPORT DOCUMENTATION PAGE I
ABSTRACT II
TABLE OF CONTENTS III
LIST OF FIGURES IV
LIST OF TABLES VI
CHAPTER 1 INTRODUCTION 1
CHAPTER 2 DROP TOWER IMPACT TEST APPARATUS 3
CHAPTER 3 EXPERIMENTAL RESULTS 6
CHAPTER 4 OBSERVATIONS 9
CHAPTER 5 CONCLUDING REMARKS AND FUTURE RESEARCH 10
REFERENCES 11
APPENDIX A DROP TOWER TEST DATA 12

LIST OF FIGURES

Figure 2.1 Scanning electron microscope images of the two granular materials tested. (a) Assembly A contains a uniform distribution of smaller particles with approximate diameter of 500 µm. (b) is the larger 1000 µm size with a split distribution……3

Figure 2.2 Drop tower test apparatus. (a) Photograph of actual equipment with labeled measurements and units. (b) A schematic with labeled components……4

Figure 2.3 Impactors used in drop tower tests. (a) Hemispherical impactor. (b) Conical impactor……5

Figure 3.1 Average penetration depths from all the drop tower tests……6

Figure 3.2 Force-displacement results for Assembly A with hemispherical impactor at initial velocity 3250 mm/s initial velocity – Test 1……7

Figure 3.3 Force-displacement results for Assembly A with hemispherical impactor at initial velocity 3250 mm/s initial velocity – Test 2……8

Figure 3.4 Force-displacement results for Assembly A with hemispherical impactor at initial velocity 3250 mm/s initial velocity – Test 3……8

Figure A.1 Force-displacement results for drop tower test using Assembly A and conical impactor at 3250 mm/s initial velocity – Test 1……13

Figure A.2 Force-displacement results for drop tower test using Assembly A and conical impactor at 3250 mm/s initial velocity – Test 2……13

Figure A.3 Force-displacement results for drop tower test using Assembly A and conical impactor at 3250 mm/s initial velocity – Test 3……14

Figure A.4 Force-displacement results for drop tower test using Assembly A and conical impactor at 4000 mm/s initial velocity – Test 1……14

Figure A.5 Force-displacement results for drop tower test using Assembly A and conical impactor at 4000 mm/s initial velocity – Test 2……15

Figure A.6 Force-displacement results for drop tower test using Assembly A and conical impactor at 4000 mm/s initial velocity – Test 3……15

Figure A.7 Force-displacement results for drop tower test using Assembly B and conical impactor at 3250 mm/s initial velocity – Test 1……16

Figure A.8 Force-displacement results for drop tower test using Assembly B and conical impactor at 3250 mm/s initial velocity – Test 2……16

Figure A.9 Force-displacement results for drop tower test using Assembly B and conical impactor at 3250 mm/s initial velocity – Test 3……..17

Figure A.10 Force-displacement results for drop tower test using Assembly B and conical impactor at 3250 mm/s initial velocity – Test 4……..17

Figure A.11 Force-displacement results for drop tower test using Assembly B and conical impactor at 3250 mm/s initial velocity – Test 5……..18

Figure A.12 Force-displacement results for drop tower test using Assembly B and hemispherical impactor at 3250 mm/s initial velocity – Test 1……..18

Figure A.13 Force-displacement results for drop tower test using Assembly B and hemispherical impactor at 3250 mm/s initial velocity – Test 2……..19

Figure A.14 Force-displacement results for drop tower test using Assembly B and hemispherical impactor at 3250 mm/s initial velocity – Test 3……..19

Figure A.15 Force-displacement results for drop tower test using Assembly B and hemispherical impactor at 4250 mm/s initial velocity – Test 1……..20

Figure A.16 Force-displacement results for drop tower test using Assembly B and hemispherical impactor at 4250 mm/s initial velocity – Test 2……..20

Figure A.17 Force-displacement results for drop tower test using Assembly B and hemispherical impactor at 4250 mm/s initial velocity – Test 3……..21

LIST OF TABLES

Table 3.1 Averaged penetration depths for all the drop tower testing scenarios…….6

Table A.1 Penetration depth for all the drop tower tests……12

CHAPTER 1
INTRODUCTION

So far, the bulk shearing behavior of granular materials under sudden shocks or impacts has eluded full understanding. The prediction of unexploded ordnance (UXO) terminal penetration depths depends on the characterization of the behavior and resulting stopping forces generated from intergranular locking and development of granular rapid-flow regimes around penetrating UXO. As a result, predictive tools available today still have to resort to continuum-based simplification of phenomenologically-observed shear resistances of the granular materials.

However, literature involving full-scale UXO penetration tests is very scarce. A combined analysis with simulations based on laboratory-scale experimental validation is an alternative for economical and thus useful means for examining the effects of UXO-soil interactions. Aside from this approach, the complexity and variability of granular geometries has obscured any deeper understanding of the underlying mechanisms behind the observed phenomena. Physics-based simplifications therefore become indispensable to accomplishing the goal of the present research.

The authors therefore commenced studying UXO impact in a systematic manner, designing granular assemblies in a controlled procedure, which lend themselves equally well to numerical analysis of UXO penetration depths as to a careful design of laboratory experiment. This report focuses on the role of such an experimental effort used to isolate geometric variances from the UXO-soil system case, thus reducing the uncertainty due to the variability of in-situ soil conditions. Such variance-isolation is investigated here by drop tests of a rigid penetrator into size-controlled granular assemblies. Experiments were carried out using a dedicated drop test facility of the Engineering Research and Development Center (ERDC) of the U.S. Army Corps of Engineers (USACE) in Vicksburg, Mississippi, which is comparable to the one put forward by Tempelman et al. (2012). Our test facility employs a guiding frame to allow free-fall drop testing of impactors with accurate control over the contact angle (i.e. the angle between the granular assembly and a reference line of the impact), with built-in wire-based sensors that are capable of measuring force-displacement time histories of the impactor.

This experiment aims to generate knowledge that is useful during the calibration and validation phase of numerical model development (apart from the experimental work itself). The post data analysis is carried out for the impactor in free-fall, which the initial impact velocity follows from the basic laws of conservation of energy, assuming that air resistance is negligible for speeds below 10,000 mm/s and relatively rigid impactor. Specifically, the test geometry, consisting of a container box with dimensions much larger (e.g., 20-25 times) than the impactor diameter (further detailed in Figures 2.2 and 2.3), will be considered as one rigid body penetrating into an unconstrained volume of granular mass from the initiation of impact (at $t = 0$) onwards. Rigid body dynamics will be utilized to compute the total vertical acceleration of the box contact point

as a function of the impact force. Next, the location of tip of the impactor will be tracked to measure a relative displacement (i.e., penetration depth) with respect to the force during contact time.

What happens during the contact time and immediately afterwards can be analyzed in the light of combined discrete element (DEM) and finite element (FEM) analysis of the impactor-granular system. Thus, a comprehensive numerical analysis on rigid body kinetics and soft particle dynamics should be conducted in the future.

CHAPTER 2
DROP TOWER IMPACT TEST APPARATUS

Two types of granular spherical particles were evaluated for particle morphology and penetration resistance. The two materials were first imaged using a FEI NovaNano SEM630 scanning electron microscope (SEM) using a low vacuum pressure to obtain an understanding of the particle morphology and size distribution (see Figure 2.1). The smaller particles were found to be on the order of 500 µm in diameter with a uniform size distribution. However, the larger particle size displayed a split distribution with some of the particles close to 1000 µm and some of them closer to 500 µm in size. The size and morphology of the two granular materials can be seen in Figure 2.1. The small and large particle size granular assemblies are referred to in this report as Assembly A and Assembly B, respectively.

After SEM imaging, the samples were tested using INSTRON CEAST 9350 Drop Tower System to empirically measure the penetration resistance of the granular material. The CEAST 9350 is a floor standing system designed to deliver up to 757 Joules (558 ft-lb) of impact energy. The standard model includes instrumentation of accelerometers, load cells, a mounted machine controller and a high-rate data acquisition system, which is suitable for a range of impact applications including tensile impact, penetration tests on plates and films, Izod, and Charpy tests. The extensive built-in instrumentation allows the engineer to obtain information that was previously unknown in geotechnical centrifuge testing, including incipient impact points. Most useful is the data of resultant load on the granular specimen that is continuously recorded as a function of time and/or specimen deflection prior to over penetration. This gives a more controlled representation of an impact than a calculated value of the geotechnical centrifuge testing set-ups.

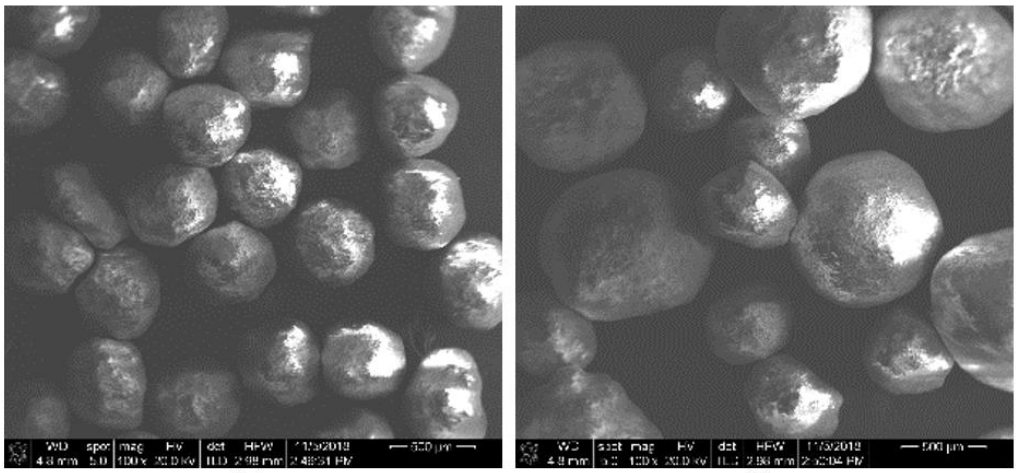

(a) (b)

Figure 2.1 Scanning electron microscope images of the two granular materials tested. (a) Assembly A contains a uniform distribution of smaller particles with approximate diameter of 500 µm. (b) is the larger 1000 µm size with a split distribution.

Figure 2.2 contains a photograph of the drop tower apparatus including relevant dimensions, along with a schematic of the relevant components. The two materials were impacted using a cone shaped impactor that went from a 12.7 mm (0.5 inches) hemisphere at its tip to a 63.5 mm (2.5 inches) base. The materials were also impacted with the hemisphere impactor. These are depicted in Figure 2.3. The tests were performed at a velocity of 3250 mm/s for all of the test with an additional 4250 mm/s for the larger particle size and the hemisphere impactor. The total weight of the impactor was measured before the testing and found to be 6.13 kg. The granular material was loaded into a container measuring 355.6 mm x 355.6 mm x 558.8 mm (14 x 14 x 22 inch) using a funnel, with a 25.4 mm opening, from a constant drop height of 26 inches from the base of the container. The container was then loaded into the drop tower via rollers to reduce settling in the material due to jostling and further compaction.

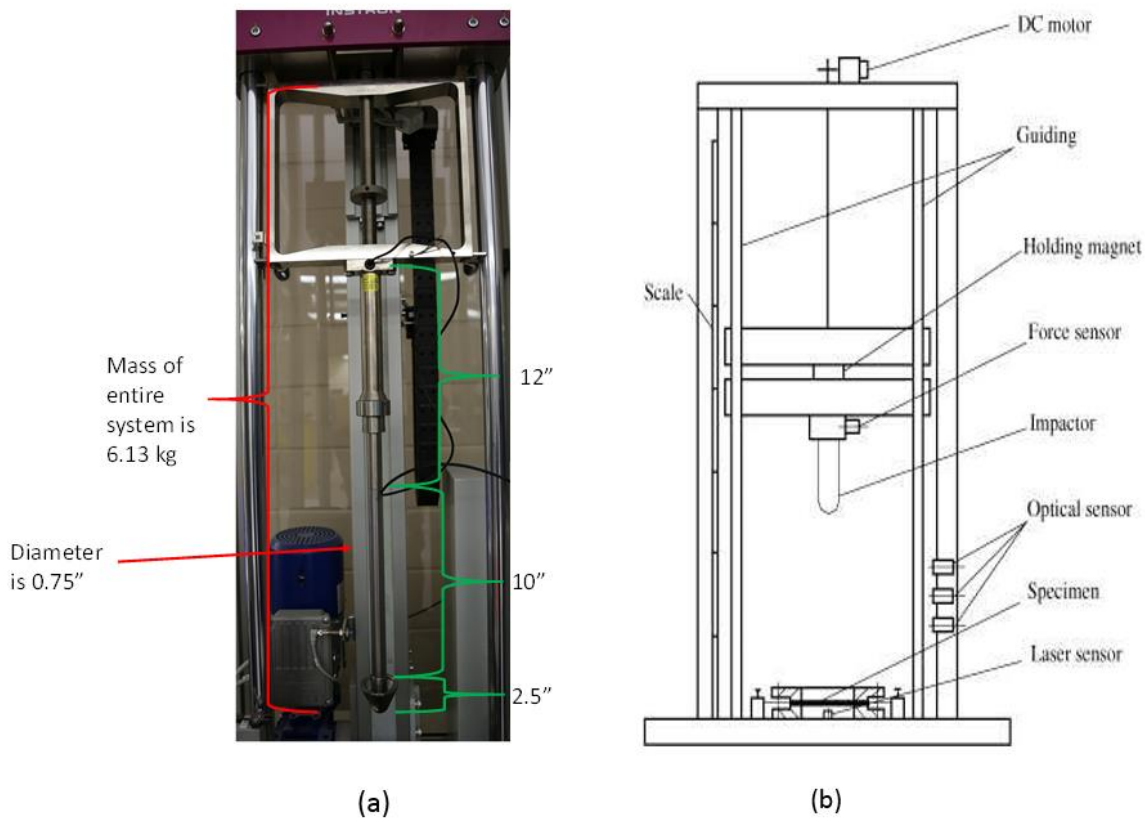

Figure 2.2 Drop tower test apparatus. (a) Photograph of actual equipment with labeled measurements and units. (b) A schematic with labeled components.

(a) (b)

Figure 2.3 Impactors used in drop tower tests. (a) Hemispherical impactor. (b) Conical impactor.

CHAPTER 3
EXPERIMENTAL RESULTS

Drop tower testing was performed on the two different granular assemblies - Assembly A: uniform distribution consisting of smaller particles (500 µm); and Assembly B: split distribution (by volume) consisting of larger particles (1000 µm) and smaller particles (500 µm). The testing matrix is intended to investigate the effects of particle sizes on penetration depth. The final penetration depth for both the assemblies is found to increase with increasing impact velocity. Two different impact velocities are prescribed to the impactor (refer to previous section for details). Three tests are conducted for each of the testing scenarios. The averaged penetration depths of drop tower tests on both assemblies are given per impactors with various nose shapes in Table 3.1, and graphically illustrated in Figure 3.1.

Table 3.1 Averaged penetration depths for all the drop tower testing scenarios

Assembly	Geometry of impactor	Initial velocity [mm/s]	Penetration depths [mm]
A	Conical	3250	96.217
		4000	174.88
B	Conical	3250	112.745
	Hemispherical	3250	99.547
		4250	183.65

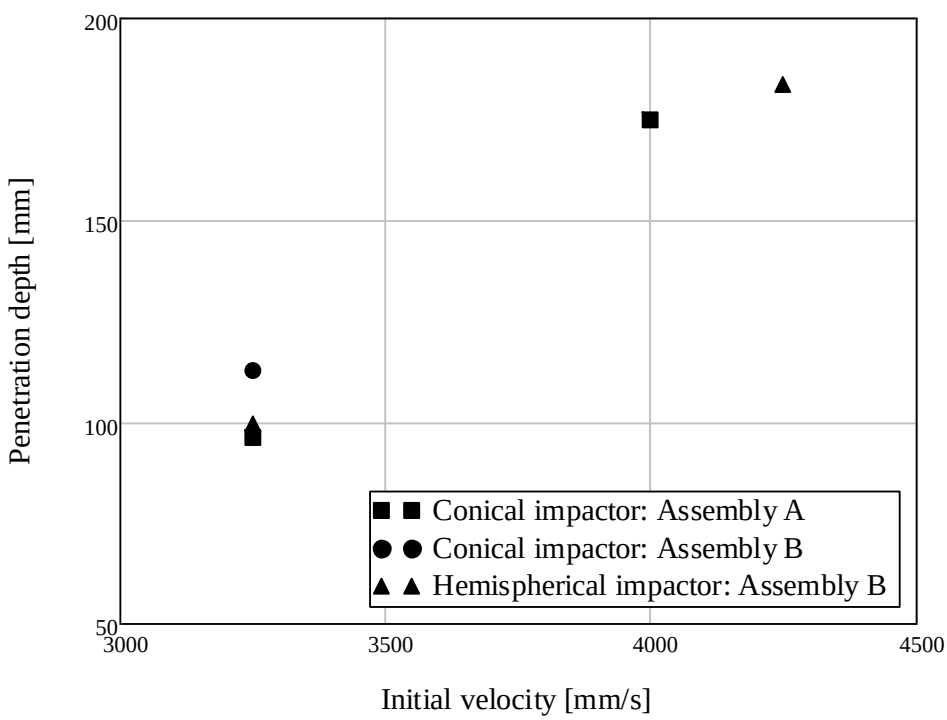

Figure 3.1 Average penetration depths from all the drop tower tests.

Resultant forces are measured as the impactor penetrates into the granular assembly. The force-displacement plots for drop tower test at 3250 mm/s initial velocity using Assembly B are given below (Figures 3.2-3.4). Oscillatory force history is observed during the penetration. Since the response of an impacted granular system strongly depends on the energy of the striking body, the initiation and propagation of elastic stress waves within a relative rigid rod of the impactor are couple with hydrodynamic behavior of granular mass flowing around the penetrating object. A one-dimensional stress wave of the impactor medium and concept of wave impedance can be analyzed along with the continuity equations of wave motion at boundary conditions for transient force, stress and velocities. Developments of semi-empirical coefficients to correlate among impact conditions can be further investigated on the use of Split Hopkinson Pressure Bar (SHPB) tests. From this experimental drop tower impact test, the dynamic stress-strain response of the granular material may be empirically examined. Therefore, a trend line is curve-fitted to the data to identify a relationship between force and displacement. The force-displacement results for all the other testing scenarios is given in Appendix A.

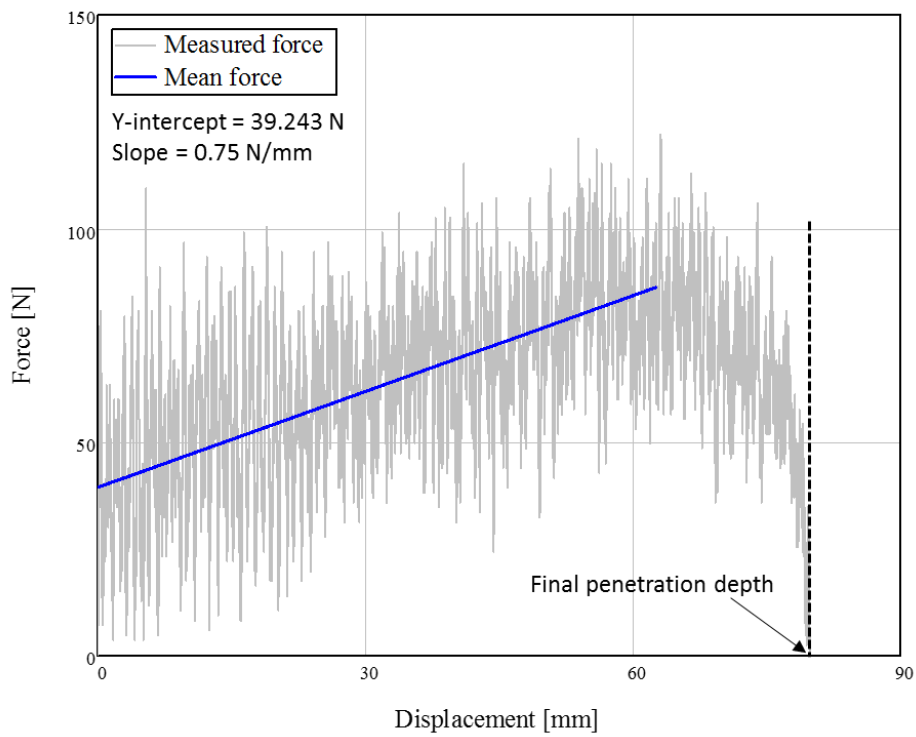

Figure 3.2 Force-displacement results for Assembly B with hemispherical impactor at initial velocity 3250 mm/s initial velocity – Test 1

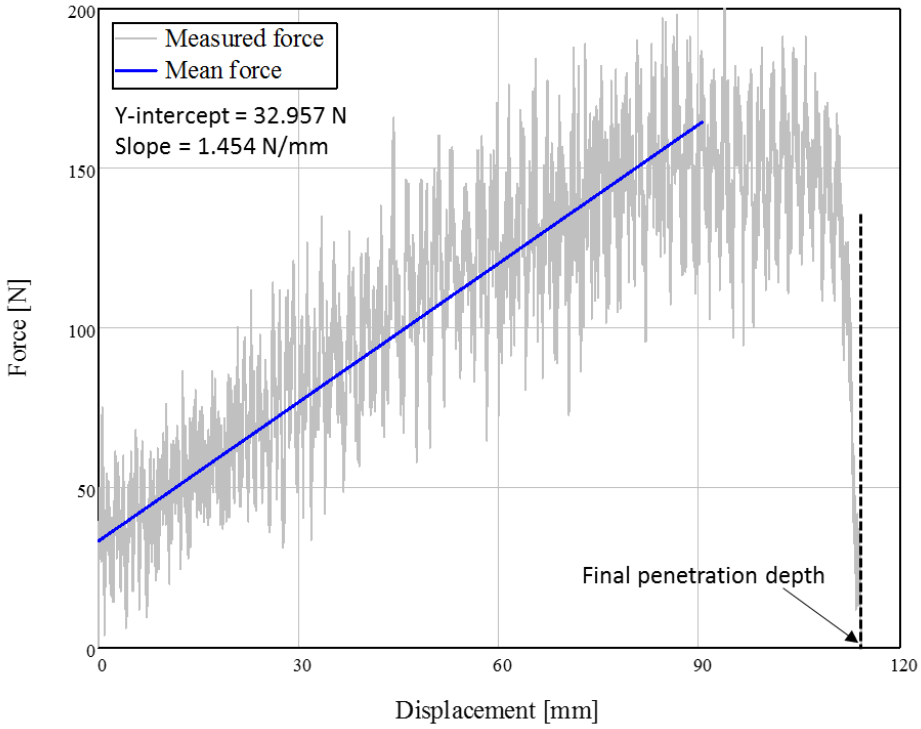

Figure 3.3 Force-displacement results for Assembly B with hemispherical impactor at initial velocity 3250 mm/s initial velocity – Test 2

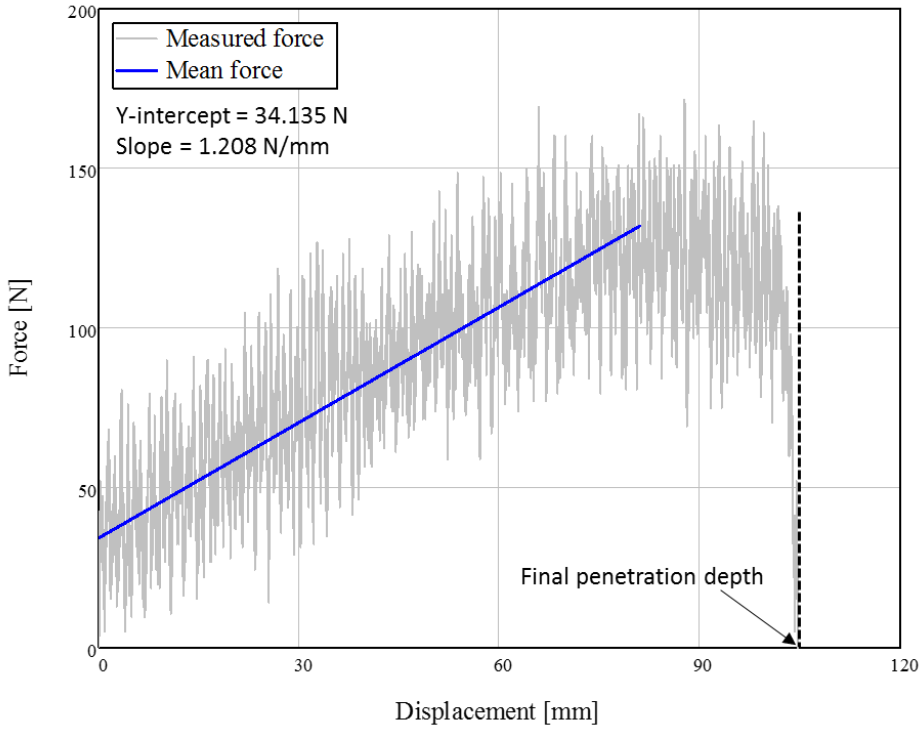

Figure 3.4 Force-displacement results for Assembly B with hemispherical impactor at initial velocity 3250 mm/s initial velocity – Test 3

CHAPTER 4
OBSERVATIONS

For each averaged penetration depth of five subsets of test results (i.e., presented in Figure 3.1), the families of data points behave in line with phenomenological observations during the geotechnical centrifuge tests. However, as the impactor transfers its momentum and kinetic energy to granules that come into contact, the patterns in momentum retardation and corresponding energy dissipation emerge to be implicitly different from one assembly to the other. For instance, a monodisperse granular assembly of the smaller granules, namely Assembly A, with mean diameter of 0.5 mm is estimated with a relatively higher values of relative density (ca. 40%) and thus results in a higher bulk shearing resistance against the penetrating impactor, while also being subjected to penetration at the lower magnitude, and the respective test produces the minimum penetration. In contrast, the binary granular assembly of larger granules (i.e., Assembly B) at a lower relative density state in a range of 20-25% possesses these larger (point) masses engaged in the penetration.

Assembly A may therefore develop a pronounced particle interlocking mechanism such that the individual grains collectively moves with nearest neighbors. It is expected to (numerically) quantify particle colloidal impact velocities relatively at a higher rate that spread over a larger region, which was observed in the numerical simulation of a prototype UXO-granular system (i.e., Chung et al. 2017). Accordingly, damping and internal forces develop for the ratios of damping and internal energies to the initial kinetic energy of the impactor. Thus, the impactor penetration retarding mechanism associated with Assembly A is influenced by the shear jamming of the smaller point mass during the initial impact and entry event.

The parametric results also indicate the presence of pronounced, consistent phenomena across all five batches of time-history plots. For example, a careful examination of the curves (Figs. A.1-A.17 of Appendix A) reveals a linear trend with respect to increasing impact velocity, which correspond to the five values of terminal penetration depth. As expected, the scale ratio of the impactors' base diameter to grain sizes is not large enough to substantiate the effect of nose shape in penetration. It is worth to note that the relative density constitutes the most substantial factor of terminal penetration depth, where volume-averaged friction value and terminal penetration depth appear to be correlated. The aforementioned observations are dictated by particle-to-impactor friction. Therefore, scale-dependent friction can be incorporated into formulation of drag and damping forces of the system, which the main stopping force components can be prescribed as transient force boundary conditions to explicitly solve the equation of motion of the impactor (e.g., UXO) and determine the terminal penetration depth using an explicit integration scheme.

CHAPTER 5
CONCLUDING REMARKS AND FUTURE RESEARCH

This report summarizes experimental findings of sub-Task 4.4 of MR 2630. Terminal penetration depth was measured in total 17 low-velocity drop tower impact tests to study the influence of the scaling in the DEM-FEM numerical prediction of UXO penetration into granular materials under lithostatic equilibrium. In all physical tests, it was seen that at lower impact energies penetration depth was strongly influenced by relative density states of granular materials. The research findings follow that modeling and analysis of maximum penetration depth require distinct description of granular materials at constituent levels which includes dynamic response and damage mechanism at high velocity impact scenarios. These advanced mesoscale DEM models are proposed for theoretical development and in-situ validation studies carried out with common munitions. Detailed code validation and subsequent simplification of the analytical procedures require further investigation in the future endeavor.

To facilitate simplified predictions of UXO terminal penetration depth, characterization of the stopping forces is of primary importance per intrinsic characteristics of soil at grain (i.e., sand) and/or microstructural (i.e., clay conglomerate) scales. Note that an inverse proportionality between frictional drag forces and terminal penetration depth has been observed in both numerical simulations and physical tests including geotechnical centrifuge scenarios of MR2630 SEED (Chung et al., 2017), which indicates a potential formulation between energy dissipation by multitudes of frictional and inertial forces (acting on grains) and corresponding kinetic energy of UXO.

Furthermore, the trend in terminal penetration depths due to increasing impact velocities is very similar in the prototype and laboratory experiments. It is also noted that the scale ratio of the projectile diameter to granule mean diameters should be further investigated beyond a margin of error equal to the standard deviation of the physical diameter of the grains at prototype scales. MR2630 numerical prediction verifies such scaling effects; the similitude parameters specific to the prototype scales used in the numerical representation of the centrifuge tests validate the scaling relation values (see the detail in Chung et al. 2017). Equally important is consistency in sample preparation of both the physical and numerical models, given the fact that the scaling relation values are found to be critical in the extrapolations across scales. Thus, it is proven to model repeatable initial and boundary conditions at the system scales, through explicit simulation of colloidal discrete particles in pluviation, both numerically and physically.

REFERENCES

Chung, J. H., Krauthammer, T., Zhang, Y., Mishra, N., Taghavi, A., Stone, M., Davidson, M., Taylor, A., Faraone, M., Patil, A., Ilay, K. (2017) "Physics-based Prediction of Unexploded Ordnance Penetration in Granular Materials," Strategic Environmental Research and Development Program (SERDP) Report, MR-2630: http://www.dtic.mil/docs/citations/AD1036286

Tempelman, E., Dwaikat, M.M.S., Spitás, C. (2012) "Experimental and Analytical Study of Free-Fall Drop Impact Testing of Portable Products," Experimental Mechanics. 52:1385-1395

APPENDIX A
DROP TOWER TEST DATA

A number of drop tower tests were performed for different sets of geometrical configurations of granular assembly, impactor geometry and impact velocity. For repeatability of tests, each testing scenario was conducted three times (five times in the case of Assembly A with conical impactor at impact velocity of 3250 mm/s). The force-displacement relationships for each drop tower test are plotted below (Figures A.1-A.17). Also, the penetration depths from all the tests are tabulated below (Table A.1). The average penetration depth for each case is plotted in Figure 3.1 in the body of the report.

Table A.1 Penetration depth for all the drop tower tests

Assembly	Geometry of impactor	Initial velocity [mm/s]	Test	Penetration depth [mm]
A	Conical	3250	1	108.47
			2	82.075
			3	98.099
			Average	**96.217**
		4000	1	171.29
			2	134.161
			3	219.176
			Average	**174.88**
B	Conical	3250	1	134.22
			2	136.48
			3	125.78
			4	79.307
			5	87.93
			Average	**112.75**
	Hemispherical	3250	1	79.815
			2	114.16
			3	104.66
			Average	**99.547**
		4250	1	208.06
			2	166.43
			3	176.45
			Average	**183.65**

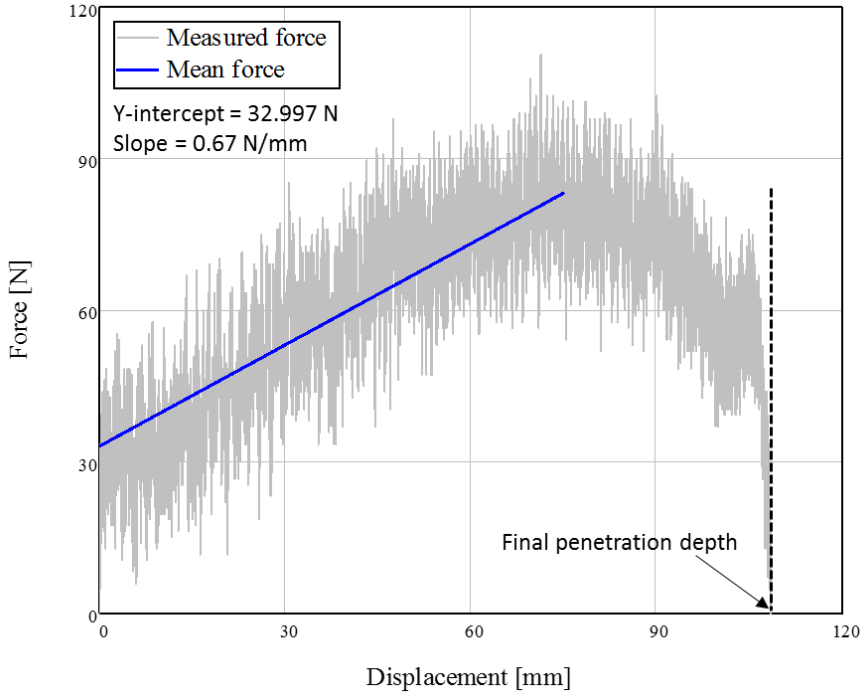

Figure A.1 Force-displacement results for drop tower test using Assembly A and conical impactor at 3250 mm/s initial velocity – Test 1

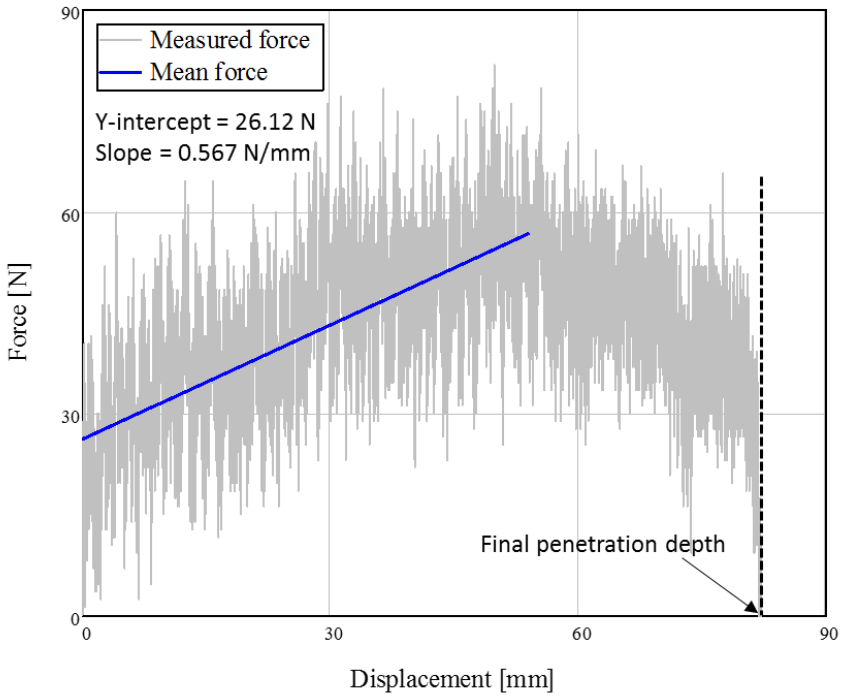

Figure A.2 Force-displacement results for drop tower test using Assembly A and conical impactor at 3250 mm/s initial velocity – Test 2

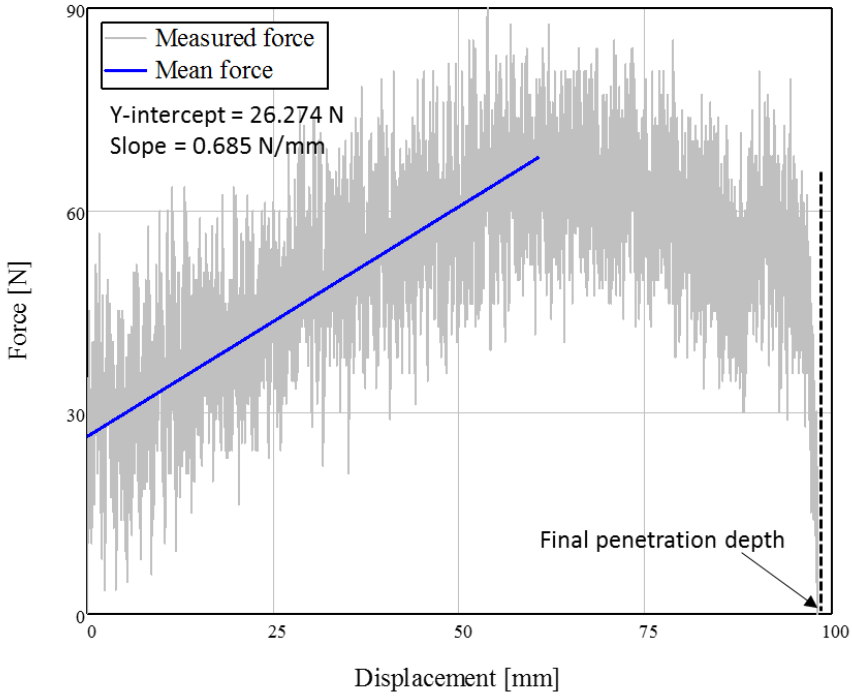

Figure A.3 Force-displacement results for drop tower test using Assembly A and conical impactor at 3250 mm/s initial velocity – Test 3

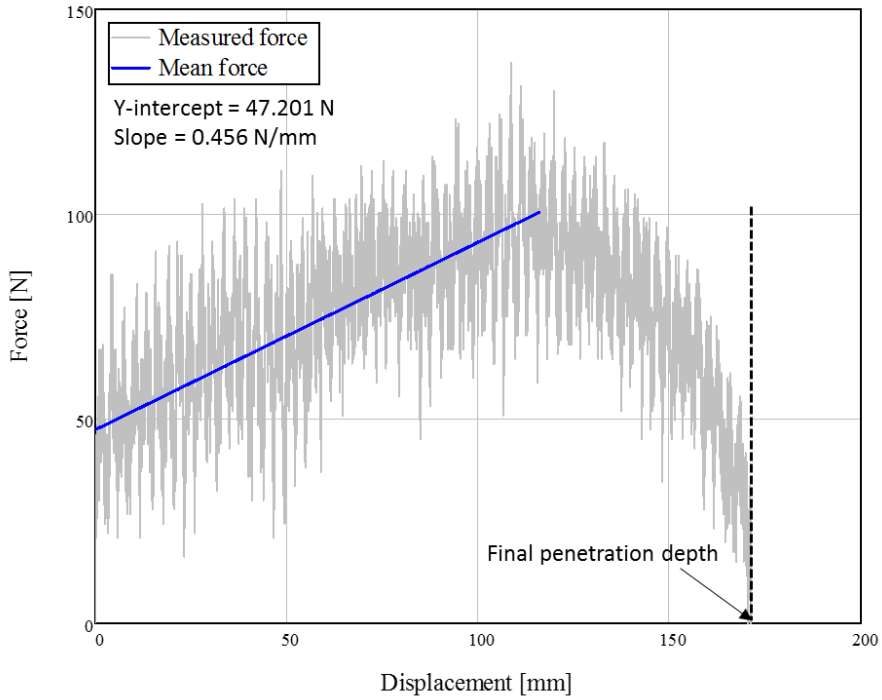

Figure A.4 Force-displacement results for drop tower test using Assembly A and conical impactor at 4000 mm/s initial velocity – Test 1

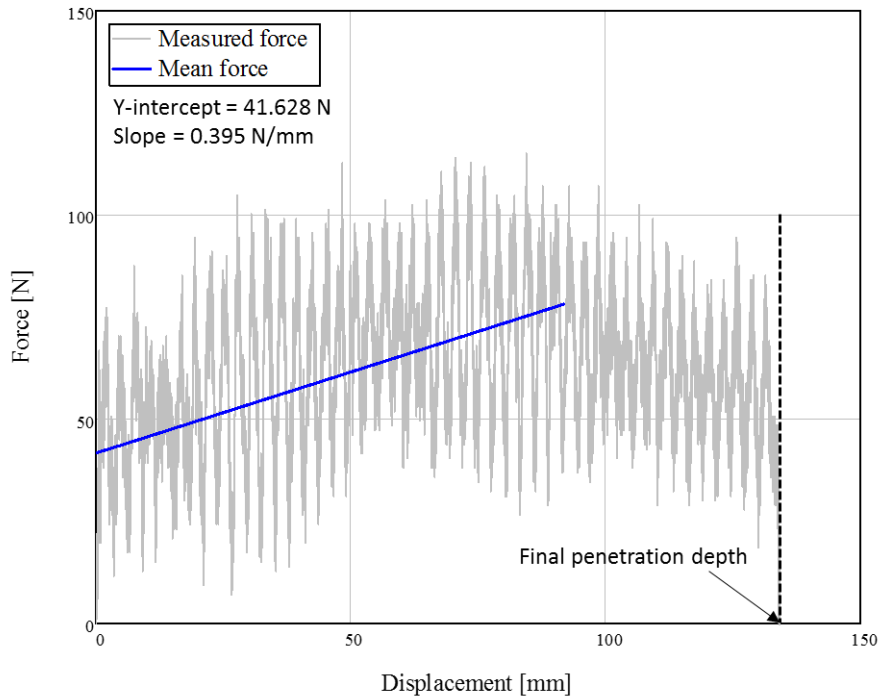

Figure A.5 Force-displacement results for drop tower test using Assembly A and conical impactor at 4000 mm/s initial velocity – Test 2

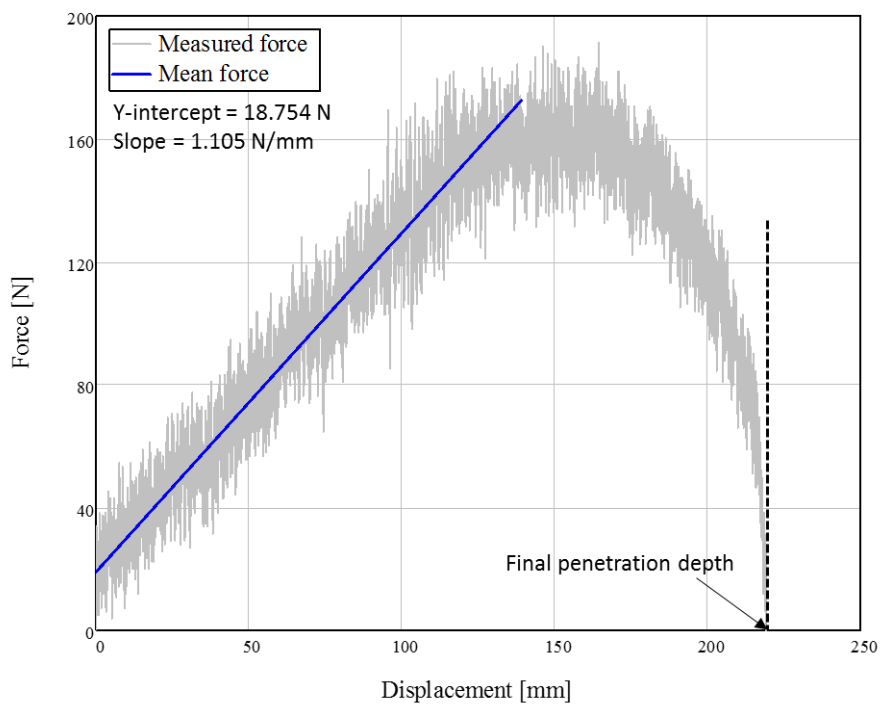

Figure A.6 Force-displacement results for drop tower test using Assembly A and conical impactor at 4000 mm/s initial velocity – Test 3

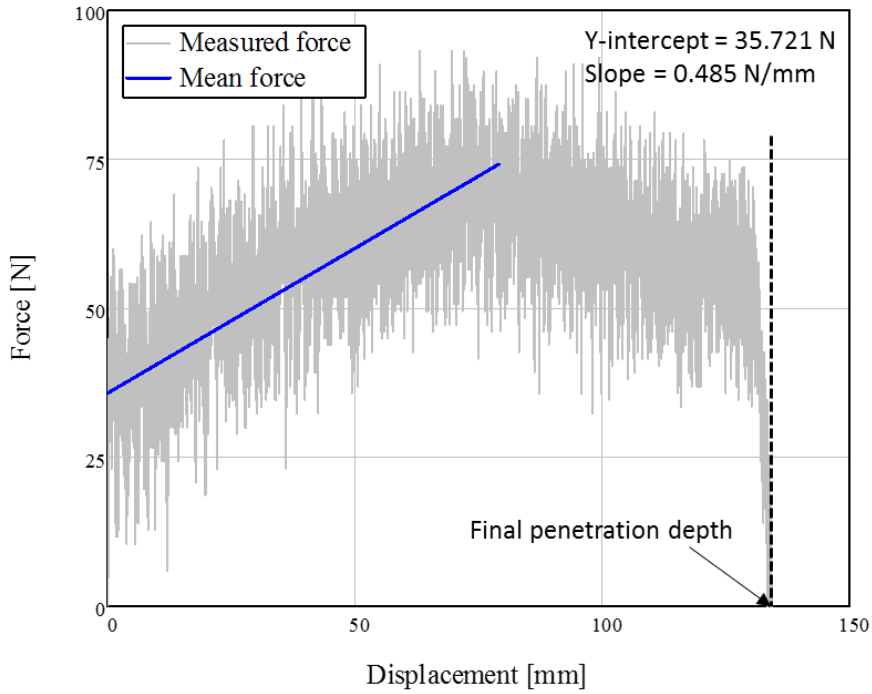

Figure A.7 Force-displacement results for drop tower test using Assembly B and conical impactor at 3250 mm/s initial velocity – Test 1

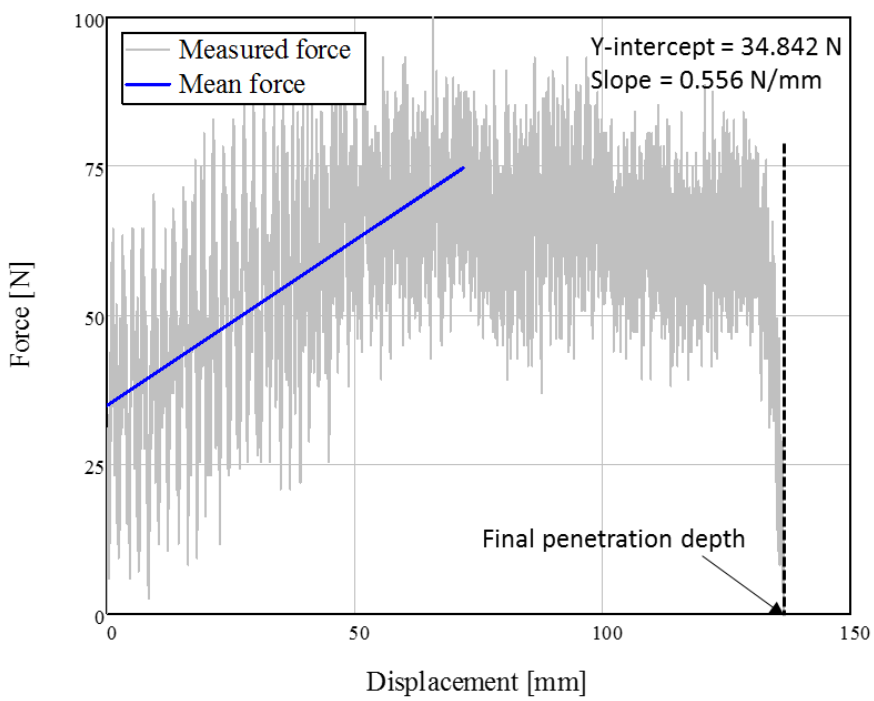

Figure A.8 Force-displacement results for drop tower test using Assembly B and conical impactor at 3250 mm/s initial velocity – Test 2

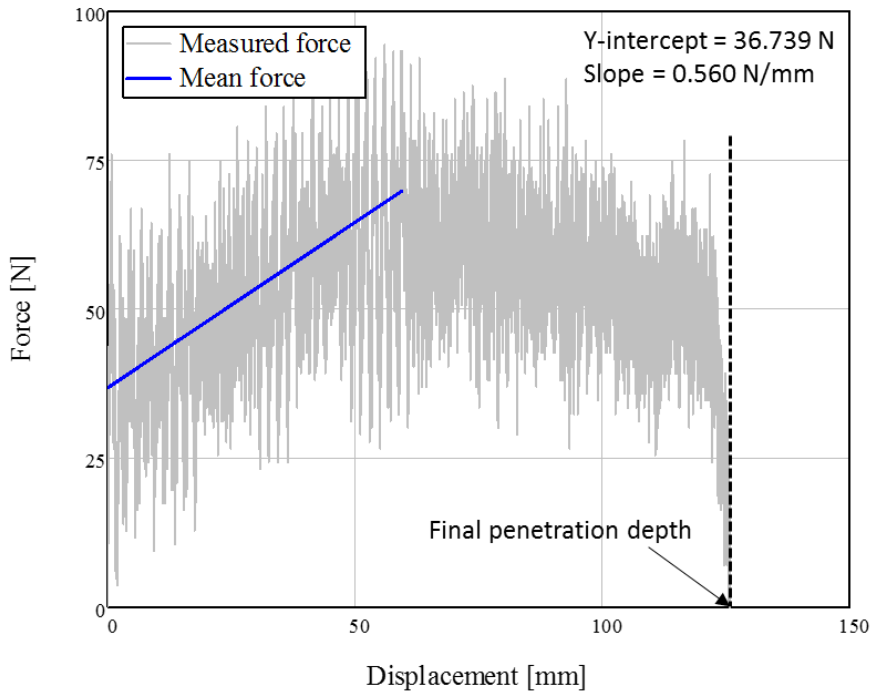

Figure A.9 Force-displacement results for drop tower test using Assembly B and conical impactor at 3250 mm/s initial velocity – Test 3

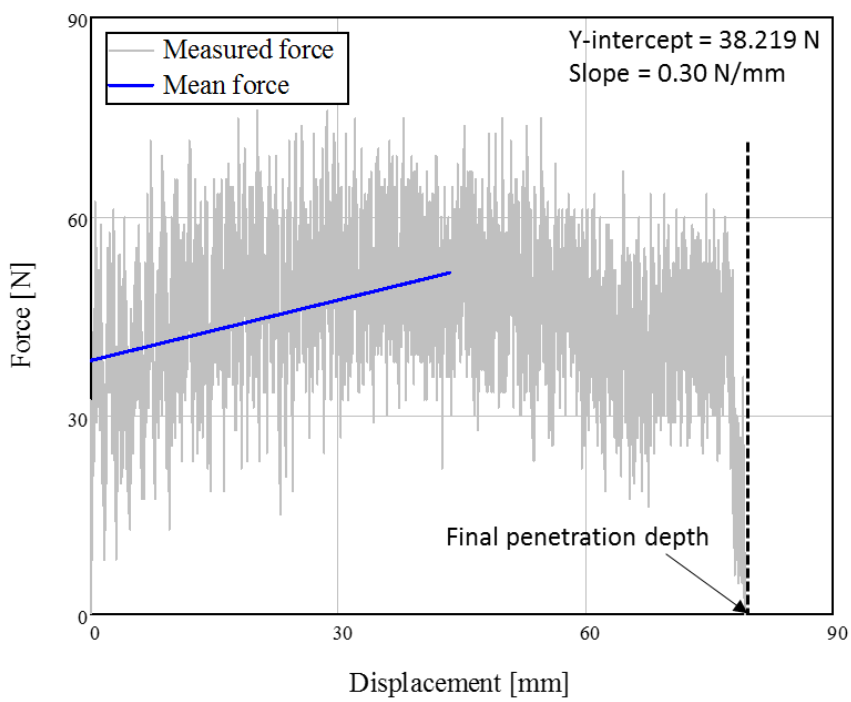

Figure A.10 Force-displacement results for drop tower test using Assembly B and conical impactor at 3250 mm/s initial velocity – Test 4

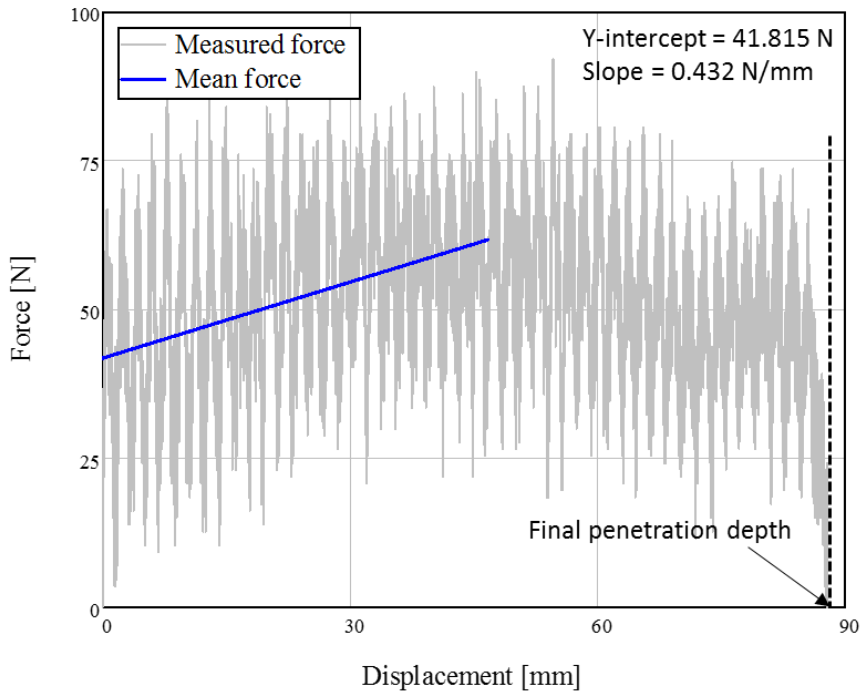

Figure A.11 Force-displacement results for drop tower test using Assembly B and conical impactor at 3250 mm/s initial velocity – Test 5

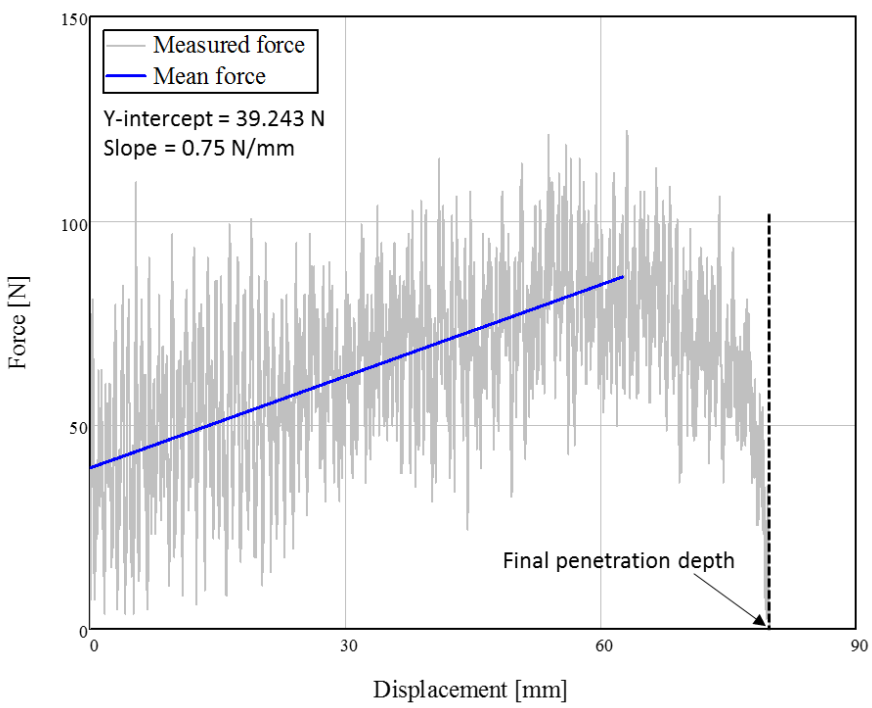

Figure A.12 Force-displacement results for drop tower test using Assembly B and hemispherical impactor at 3250 mm/s initial velocity – Test 1

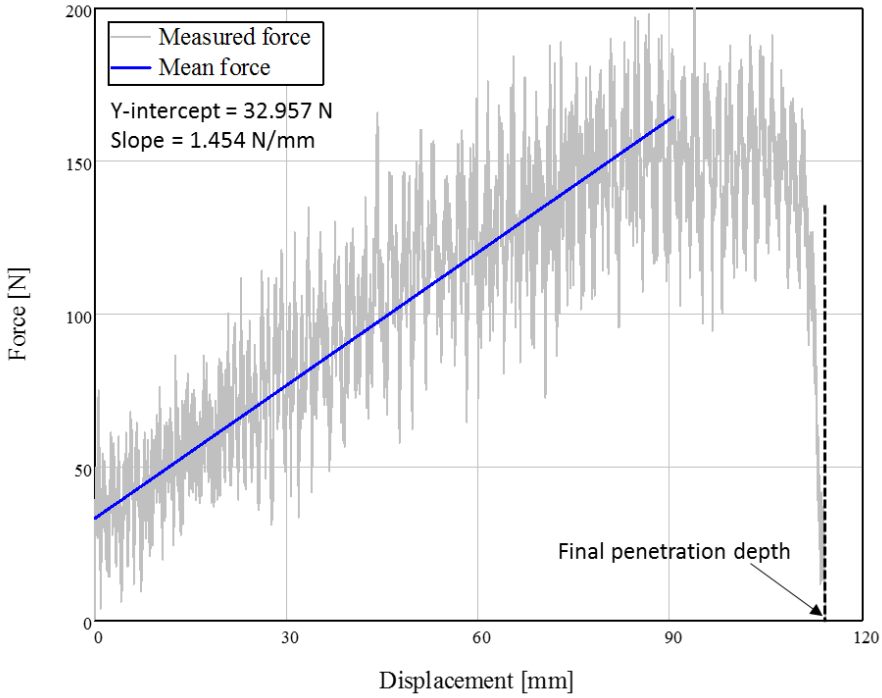

Figure A.13 Force-displacement results for drop tower test using Assembly B and hemispherical impactor at 3250 mm/s initial velocity – Test 2

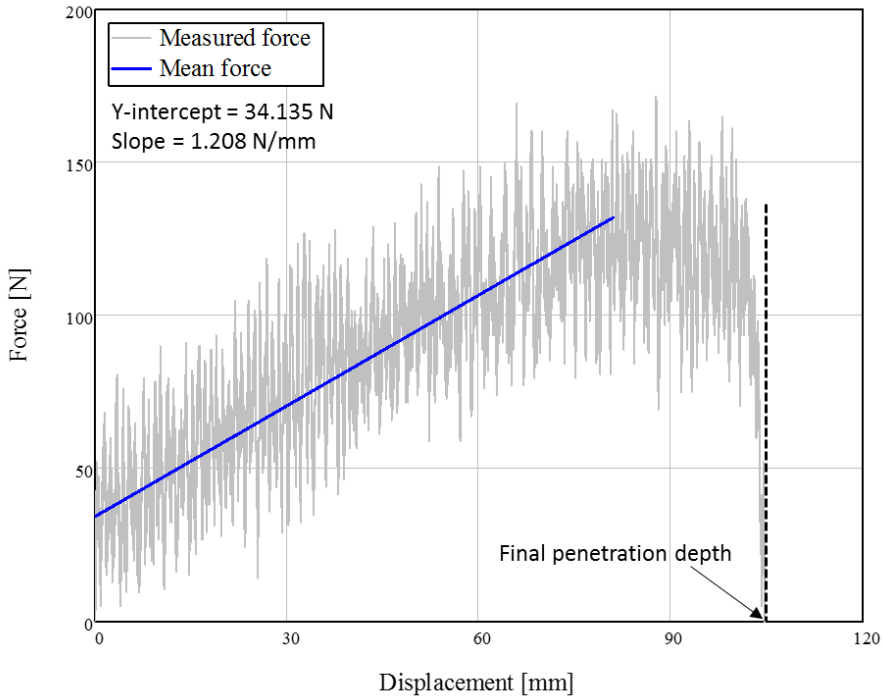

Figure A.14 Force-displacement results for drop tower test using Assembly B and hemispherical impactor at 3250 mm/s initial velocity – Test 3

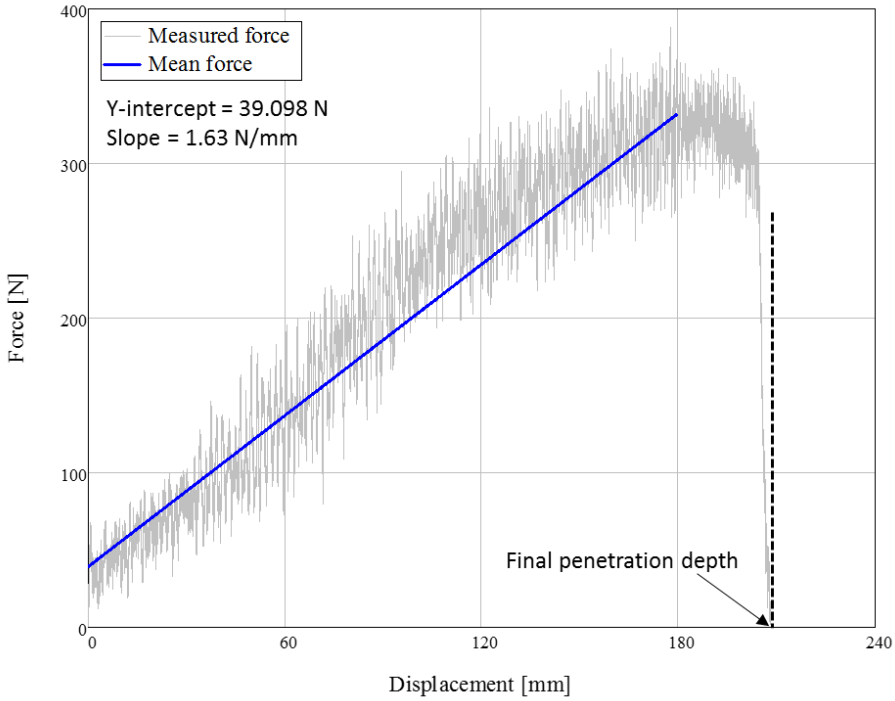

Figure A.15 Force-displacement results for drop tower test using Assembly B and hemispherical impactor at 4250 mm/s initial velocity – Test 1

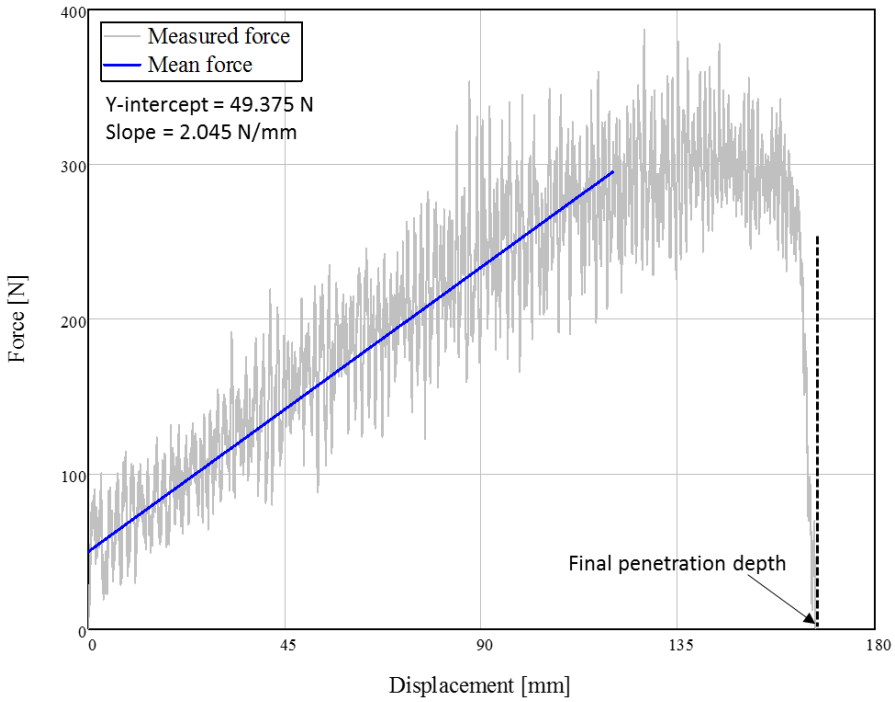

Figure A.16 Force-displacement results for drop tower test using Assembly B and hemispherical impactor at 4250 mm/s initial velocity – Test 2

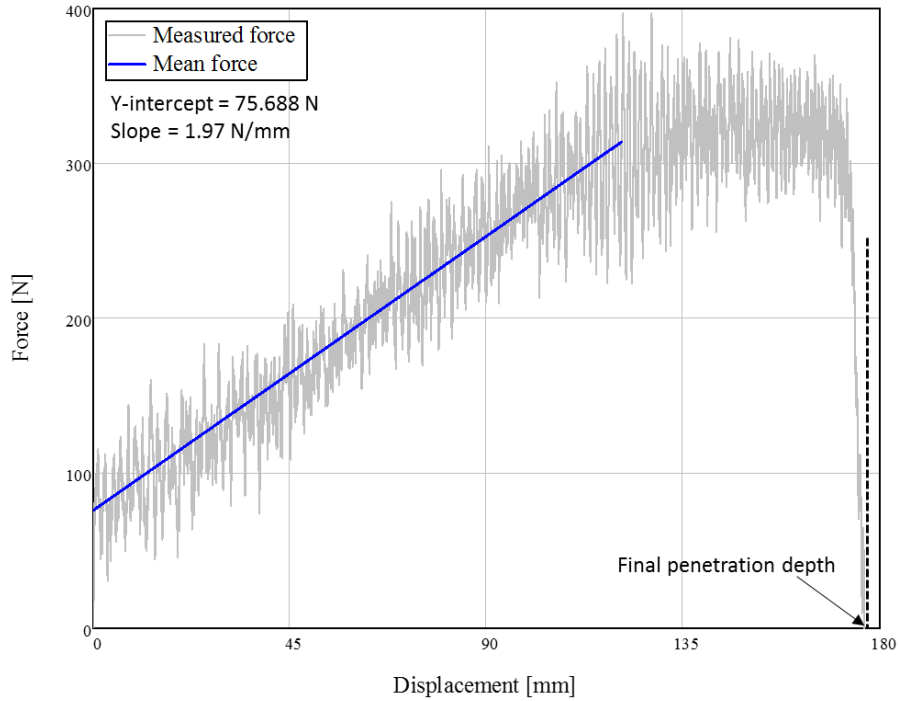

Figure A.17 Force-displacement results for drop tower test using Assembly B and hemispherical impactor at 4250 mm/s initial velocity – Test 3